ELSEVIER

Materials Science and Engineering A 412 (2005) 279–286

MATERIALS SCIENCE & ENGINEERING A

www.elsevier.com/locate/msea

Cyclic deformation and fatigue properties of Al–0.7 wt.% Cu alloy produced by equal channel angular pressing

Z.F. Zhang *, S.D. Wu, Y.J. Li, S.M. Liu, Z.G. Wang

Shenyang National Laboratory for Materials Science, Institute of Metal Research, Chinese Academy of Sciences, 72 Wenhua Road, Shenyang 110016, PR China

Accepted 31 August 2005

Abstract

Fatigue damage behavior of an Al–0.7 wt.% Cu alloy, produced by equal channel angular pressing (ECAP) technique, was investigated under constant plastic strain control. It showed that the Al–0.7 wt.% Cu alloy displayed obvious cyclic softening at all the strain amplitudes. The cyclic softening can be attributed to a combination of higher yield strength and hysteresis energy density than the original material. The plastic deformation was carried out by shear bands at low or medium strain ranges, or by both shear bands and coarse deformation bands at high strain ranges. Consequently, fatigue cracks nucleated either along shear bands or along the coarse deformation bands, depending on the applied strain amplitude.

Keywords: Equal channel angular pressing (ECAP); Al–0.7 wt.% Cu alloy; Cyclic softening; Hysteresis energy density; Shear bands; Deformation bands; Fatigue crack

1. Introduction

Ultra-fine grained (UFG) materials possess many unusual properties such as high strength [1], high stress fatigue life [2–4] and super-plastic deformation ability [5] at low temperature, etc., and thus have become one of the hot topics in the field of advanced structural materials [6]. At present, among all of the methods to obtain the UFG materials, equal channel angular pressing (ECAP) technique is especially attractive and has been widely applied to various metals and alloys by many investigators [7] in the world. To date, many investigations have focused on the static mechanical properties of the UFG materials such as uniaxial tensile or compressive tests, however, the study on fatigue properties is quite rare, mainly on pure Cu [3,4,8–11], Al alloys [4,12–15] and *a few other metals* or alloys [16–20]. In *most UFG metals* [4,9–11] and alloys [2,15,16,20], one of the pronounced features is cyclic softening during strain fatigue. Besides, another common phenomenon is the formation of localized shear bands, which are also the precursors to fatigue cracking in some wavy-like UFG materials [4,10,13,14,16,18]. As well known in conventional metallic materials, fatigue cracking is often controlled by several factors such as slip bands, grain or twin boundaries, second phases or voids. However, the understanding of fatigue damage and cracking mechanisms in such kind of materials is rare and poor; therefore, it is necessary to learn whether there is a new mechanism controlling the failure of the UFG materials or not. In the present work, we report the cyclic deformation and fatigue properties of an Al–0.7 wt.% Cu alloy subjected to severe plastic deformation. It is expected that the addition of Cu element will further improve the strength on the base of the ECAPed pure Al due to the precipitation strengthening effect of the Al–Cu phase [21]. Moreover, the cyclic stress response and fatigue cracking mechanism of the Al–0.7 wt.% Cu alloy are discussed.

2. Experimental procedure

Al–0.7 wt.% Cu alloy was employed in this study for severe plastic deformation. First, the alloy ingot was cut into some bars with a dimension of Ø 10 mm × 80 mm and then annealed at 550 °C for 84 h. The bars were subjected to multiple pressing through an ECAP die with two round channels intersecting at 90°. Most samples were pressed for 4 passes at room temperature via the so-called route C. After ECAP treatment, the

* Corresponding author. Tel.: +86 24 23971043; fax: +86 24 23891320.
E-mail address: zhfzhang@imr.ac.cn (Z.F. Zhang).

0921-5093/$ – see front matter © 2005 Published by Elsevier B.V.
doi:10.1016/j.msea.2005.08.221

samples were cut into tensile and fatigue specimens with a gauge size of 5 mm × 5 mm × 16 mm. Before mechanical tests, all the specimens were electrolytically polished to produce a strain-free surface for microscopic observation. The specimens for tensile tests were pressed for 2, 3, or 4 passes; while *all the specimens* for fatigue tests *were pressed* for 4 passes. Cyclic deformation was performed in push–pull mode on a Shimadzu servo-hydraulic testing machine under constant plastic strain control at room temperature in air. Most specimens were cycled to failure for the measurement of their fatigue life. However, for some specimens, cyclic deformation was interrupted at different cycles, then the surfaces of those specimens were observed under a Cambridge S360 scanning electron microscope (SEM) to examine deformation morphology and fatigue-cracking features.

3. Results and discussion

3.1. Tensile and cyclic stress responses

Fig. 1 shows the tensile stress–strain curves of the specimens subjected to 2- or 4-pass ECAP treatment. It can be seen that the yield strength is about 142.2 MPa (2-pass ECAP) and 182.4 MPa (4-pass ECAP), respectively, indicating that higher ECAP pass obviously increases the yield strength. Meanwhile, it is noted that the elongation of 4-pass ECAP is a little bit higher than that of 2-pass ECAP. It indicates that, at certain conditions, the yield strength and elongation of the Al–0.7 wt.% Cu alloy can be enhanced simultaneously by ECAP treatment. To reveal the effect of Cu element, some data of pure Al subjected to ECAP treatment is employed. For example, Zheng [22] found that the yield strength of commercial pure Al was about 65.7 MPa (no ECAP), 104.4 MPa (2-pass ECAP) and 139.5 MPa (4-pass ECAP), respectively. Therefore, the difference in the yield strength between Al–0.7 wt.% Cu and pure Al is 37.8 MPa (2-pass ECAP) and 42.9 MPa (4-pass ECAP). This indicates that adding a small amount of Cu element can also obviously improve the strength of the Al alloy besides the ECAP treatment. The strengthening mechanism of Cu element should be attributed to the precipitation of the θ phase in Al–Cu alloy [21] and will be further revealed *elsewhere* [23].

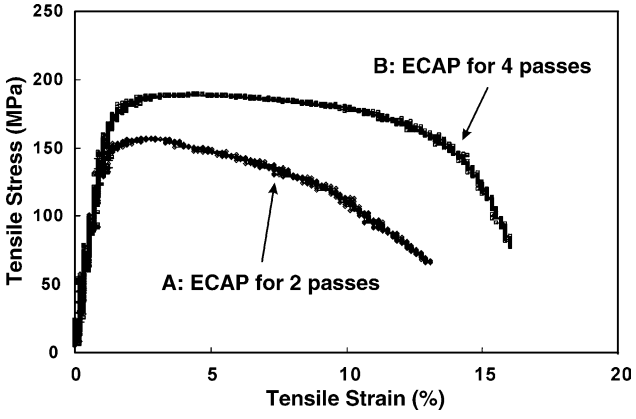

Fig. 1. Tensile stress–strain curves of the Al–0.7 wt.% Cu alloy subjected to severe plastic deformation.

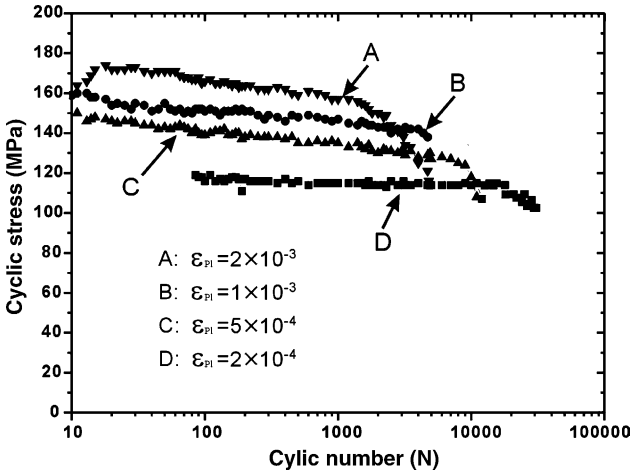

Fig. 2. Cyclic stress response of the Al–0.7 wt.% Cu alloy subjected to 4-pass ECAP treatment.

Fig. 2 shows the cyclic stress response of the Al–0.7 wt.% Cu alloy subjected to 4-pass ECAP treatment in the plastic strain range of 2×10^{-4} to 2×10^{-3}. It can be seen that all the specimens display obvious cyclic softening behavior under the applied strain range. The cyclic softening ratio, as defined as by Hoppel et al. [9], increases with increasing strain amplitude. The present cyclic softening feature is well consistent with the reports on many other UFG materials [2,4,9–11,15,16,20]. For a better comparison, the cyclic stress responses of the available metals and alloys subjected to ECAP treatment are summarized in Table 1. A very pronounced feature in those materials is that cyclic softening nearly occurs in *all the* ECAPed metals or alloys [2,4,9,10,15,16,20] except for few examples of cyclic saturation or hardening behavior [11,13,14,17]. It can be concluded that *most metals* or alloys subjected to severe plastic deformation are prone to cyclic softening during strain fatigue.

3.2. Cyclic stress–strain curves and fatigue life

Since the Al–0.7 wt.% Cu alloy always exhibits apparent cyclic softening at the applied strain range, it is very difficult

Table 1
Fatigue features of various metals and alloys subjected to severe plastic deformation

Authors	Materials	Fatigue features
Chung et al. [2]	6061 Al	Softening
Vinogradov and Hashimoto [4]	Cu	Softening
Hoppel et al. [9]	Cu	Softening
Wu et al. [10]	Cu	Softening
Mughrabi et al. [11]	α-Brass	Saturation
	Cu	Softening
	Al	Softening
Liu and Wang [15]	8090 Al	Softening
Vinogradov et al. [16]	Fe–36Ni	Softening
Kim et al. [20]	Low carbon steel	Softening
Patlan et al. [13]	5056 Al–Mg	Saturation
Vinogradov et al. [14]	Al–Mg–Sc–Zr	Saturation or hardening
Vinogradov et al. [17]	Ti	Saturation

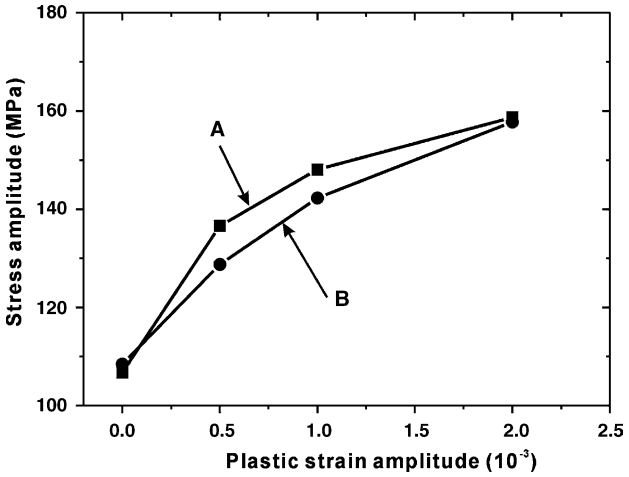

Fig. 3. Cyclic stress–strain curves of the Al–0.7 wt.% Cu alloy subjected to 4-pass ECAP treatment: (A) represents the average stress and (B) represents the half-life stress.

to give a cyclic stress–strain curve, as reported in *single-*, *bi-* or *poly-crystals* [24–26]. In the present study, two stresses are employed, i.e. stress $\sigma_{N_f/2}$ at half fatigue life and average stress $\sigma_{mean} = (\sum_{i=1}^{N_f}\sigma_i)/N_f$ for all the cycles. Therefore, the defined cyclic stress–strain curves of the 4-pass ECAPed specimens are plotted in Fig. 3. It can be seen that the stress rapidly increases with the applied strain amplitude. Meanwhile, the average stress σ_{mean} (line A) is a little bit higher than the stress $\sigma_{N_f/2}$ (line B) at half fatigue life, indicating that cyclic softening is more pronounced before half-life cycles.

The curves of fatigue life $2N_f$ versus applied plastic strain amplitude ε_{pl} are plotted in Fig. 4, as well as two other Al alloys subjected to ECAP treatment. It is apparent that the fatigue life of the Al–0.7 wt.% Cu alloy is higher than those of Al–1.5Mg–Sc–Zr and Al–6Mg–0.5Sc–0.15Zr alloys [13,14]. According to Coffin–Manson law, one knows

$$\varepsilon_{pl} = \varepsilon_f(2N_f)^c \tag{1}$$

where ε_f is the fatigue ductile coefficient and c is the fatigue ductile exponent. From Fig. 4, the two constants can be calculated as $\varepsilon_f = 3.60$ and $c = -0.903$ for the Al–0.7 wt.% Cu alloy. Therefore, *the fatigue life* N_f can be expressed as a function of the applied plastic strain amplitude ε_{pl}, i.e.

$$N_f = \frac{(3.6/\varepsilon_{pl})^{1.1}}{2} \tag{2}$$

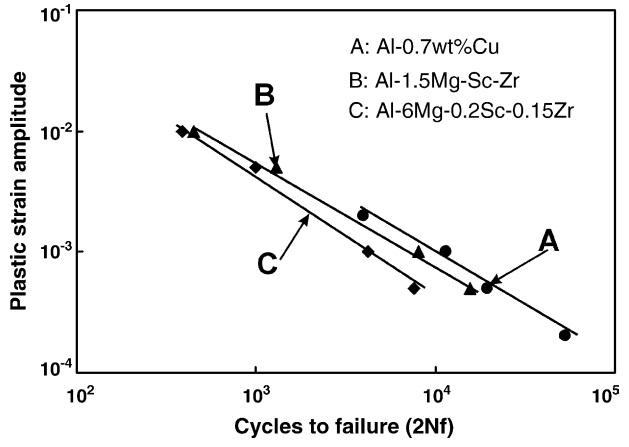

Fig. 4. Relationship of the plastic strain amplitude vs. fatigue life $2N_f$ of the Al–0.7 wt.% Cu alloy and other two Al alloys subjected to ECAP treatment.

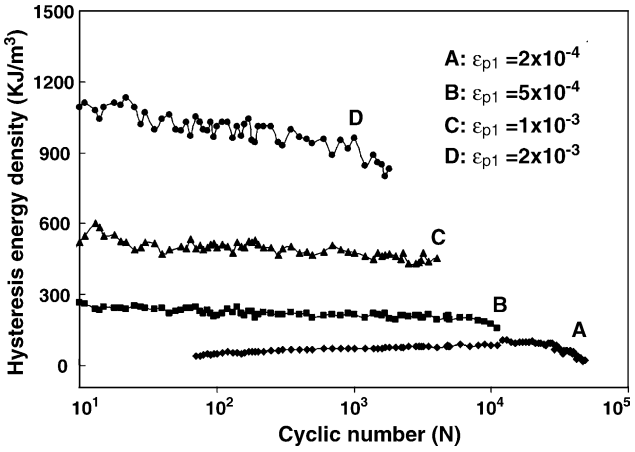

Fig. 5. Variation of hysteresis energy density with cyclic number at different strain amplitudes.

3.3. Hysteresis energy induced by cyclic deformation

During cyclic deformation, the stress–strain curve per cycle can form a closure loop, whose area ΔW_a represents the applied hysteresis energy density to the specimen. Wherein

$$\Delta W_a = \oint \sigma \, d\varepsilon \tag{3}$$

As shown in Fig. 5, the variation of ΔW_a versus cyclic number is plotted. It can be seen that ΔW_a nearly remains constant at low strain amplitude; however, it displays obvious instability at high strain amplitude. For comparison, the average hysteresis energy density ΔW_{mean} per cycle at each strain amplitude was calculated as

$$\Delta W_{mean} = \frac{\sum_{i=1}^{i=N_f}\Delta W_{ai}}{N_f} \tag{4}$$

During cyclic deformation, the applied average hysteresis energy E_{mean} per cycle to a specimen can be expressed as

$$E_{mean} = \Delta W_{mean} V \tag{5}$$

where V is the volume of the deformed specimen. For the Al–0.7 wt.% Cu alloy, if there is a temperature increase ΔT, the absorbed energy E will be equal to

$$E = C\rho V \, \Delta T \tag{6}$$

where $C = 8.9 \times 10^2$ J/kg K is the specific heat of the Al–0.7 wt.% Cu alloy and $\rho = 2.7 \times 10^3$ kg/m^3 is the density of the Al–0.7 wt.% Cu alloy. In an ideal situation, if all the energy E_{mean} per cycle contributes to the temperature increase ΔT of the deformed volume V, one can set up the following balance

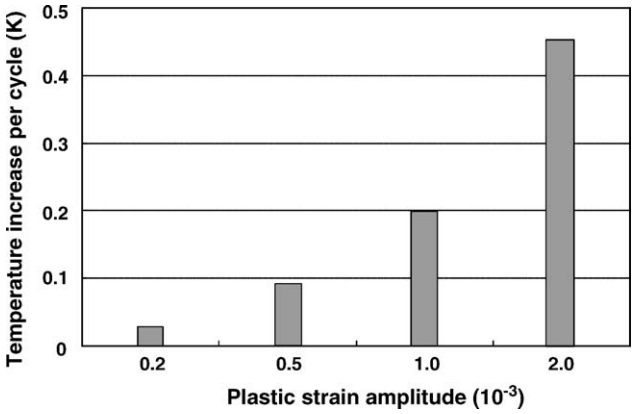

Fig. 6. Possible temperature increase induced by hysteresis energy per cycle at different strain amplitude.

between Eqs. (5) and (6):

$$\Delta W_{\text{mean}} V = C\rho V\,\Delta T \tag{7}$$

Therefore, the possible temperature increase ΔT can be expressed as

$$\Delta T = \frac{\Delta W_{\text{mean}}}{C\rho} \tag{8}$$

According to Eq. (8), if all the energy E_{mean} is transformed into heat of the deformed specimen, the possible temperature increase ΔT per cycle at different strain amplitude can be calculated and is plotted in Fig. 6. It is shown that the maximum temperature increase ΔT per cycle is about 0.45 °C at $\varepsilon_{\text{pl}} = 2 \times 10^{-3}$, and about 0.022 °C at $\varepsilon_{\text{pl}} = 2 \times 10^{-4}$. This means that ΔT must be very pronounced at $\varepsilon_{\text{pl}} = 2 \times 10^{-3}$ if all the energy E_{mean} is fully transformed into heat at the end of fatigue.

On the other hand, it is well known that the flow stress of the ductile material without ECAP treatment must be obviously lower than that of the ECAPed material, as illustrated in Fig. 7. Accordingly, ΔW_{mean} per cycle of the materials without ECAP treatment (loop B) will be greatly smaller than that of the

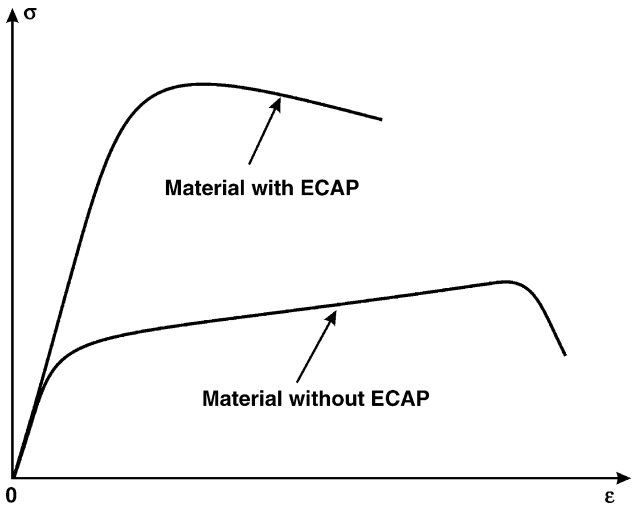

Fig. 7. Illustration of the tensile stress–strain curves in the materials with and without ECAP treatment.

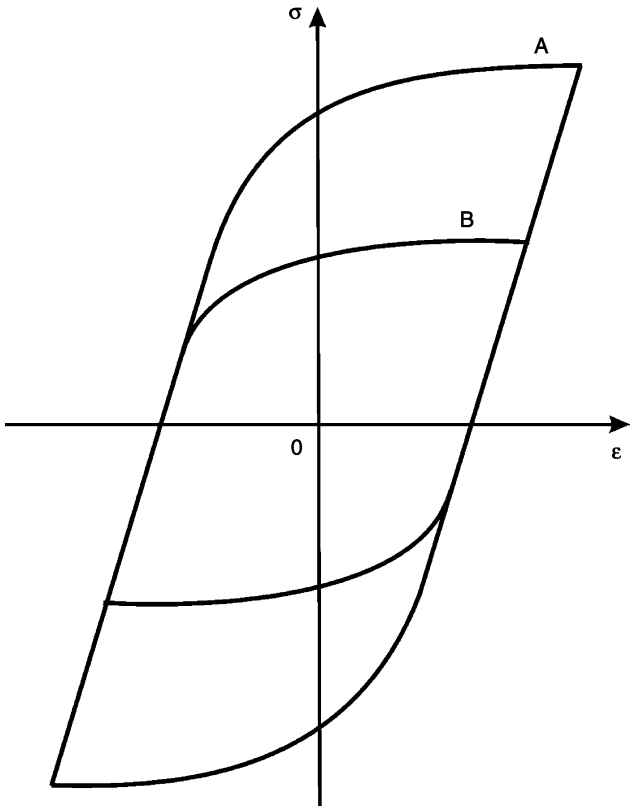

Fig. 8. Illustration of the hysteresis loops in the materials with and without ECAP treatment: (A) ECAPed materials and (B) conventional material.

ECAPed material (loop A), as illustrated in Fig. 8. Meanwhile, the materials subjected to severe plastic deformation usually contain a certain amount of dislocations and defects, *most energy* W_{mean} *will be* used to drive the movement and annihilation of dislocations and defects, even grain boundaries sliding and shear deformation rather than the temperature increase, during cyclic deformation. However, the energy density ΔW_{mean} of the materials without ECAP treatment is usually used to produce more dislocations or defects during cyclic deformation. Therefore, E_{mean} does not produce a temperature increase ΔT, but is used to drive the movement and annihilation of dislocations. Accordingly ΔT can only be regarded as a qualitative parameter for describing the possibility of cyclic softening or not in the UFG materials. In other words, the possible trend should be cyclic softening for the ECAPed materials, and cyclic hardening for the ductile materials without ECAP treatment.

Finally, the reason for cyclic softening might be associated with the tensile stress–strain curve feature of the UFG materials, as seen in Fig. 7. In general, the tensile stress–strain curves in most of the UFG materials often display the following features. After yielding, the materials always exhibit obvious softening or stable plastic flow without work hardening. It indicates that the UFG materials have lost the potential for further strain strengthening after many-pass ECAP treatment. As a result, the occurrence of cyclic softening is unavoidable. For example, in some Al–Mg–Sc–Zr alloys subjected to ECAP treatment [14], when their tensile stress–strain curves display an ability of work hardening, its cyclic stress response can behave in a cyclic satu-

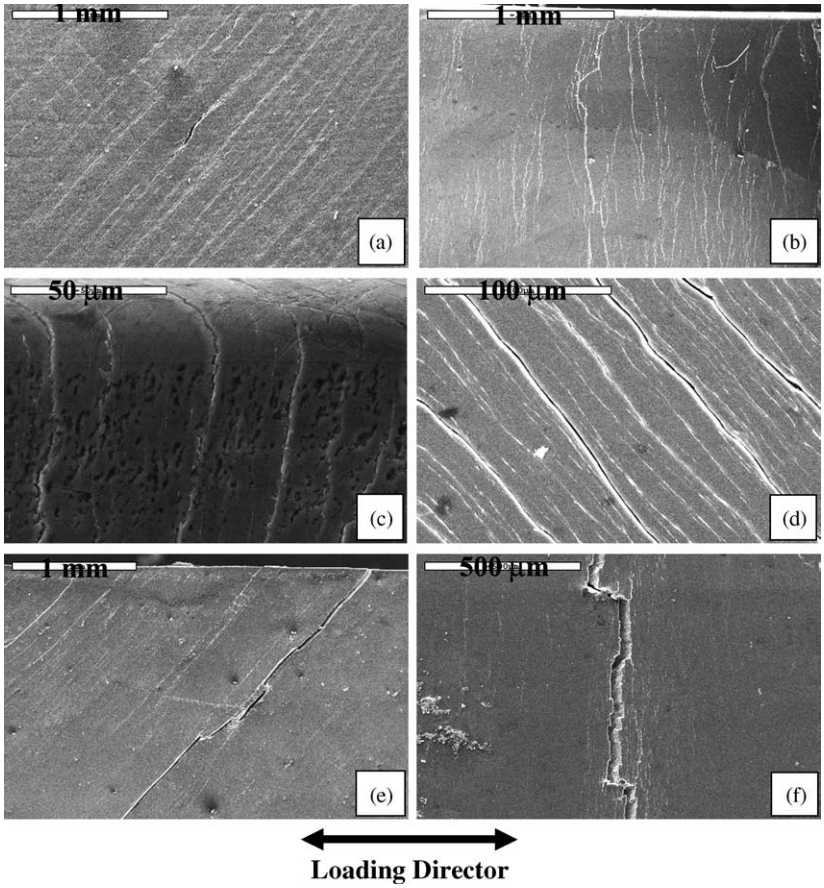

Fig. 9. Shear deformation and fatigue cracking behavior in the ECAPed Al–0.7 wt.% Cu alloy at the plastic strain amplitude below 10^{-3}.

ration manner (Al–4.5Mg–Sc–Zr and Al–1.5Mg–Sc–Zr), even cyclic hardening (Al–6Mg–Sc–Zr). Therefore, it is suggested that the widely observed cyclic softening in the UFG metals and alloys can be attributed to the following reasons: (i) a relatively higher hysteresis energy density per cycle (due to high strength) than that in the materials without ECAP treatment; (ii) a softening or stable deformation feature in the tensile stress–strain curves (no potential ability for strain strengthening); (iii) existence of amounts of dislocations and defects after ECAP treatment.

3.4. Deformation and damage features

Fig. 9 shows typical deformation morphology of the Al–0.7 wt.% Cu alloy fatigued at the plastic strain amplitude below 10^{-3}. It can be seen that there are many long and straight shear bands, which is quite similar to persistent slip bands in fatigued copper single crystals [27]. On one surface of the specimen, the shear bands make an angle of around 45° with respect to the stress axis, as shown in Fig. 9(a). On the adjacent surface, the shear bands are nearly perpendicular to the loading direction (see Fig. 9(b)). This indicates that the shear bands should approximately occur along the maximum shear stress plane of the specimen, which was also observed in other UFG metals or alloys with wavy-like slip, such as Cu [10], Fe–36Ni [16] and Cu–Zr–Cr alloys [18]. Meanwhile, it is noted that the shear bands do not change their direction and can transfer through the whole specimen, which is quite different from the random distribution of slip bands in coarse grain materials [28]. It demonstrates that the ultra-fine grains in the specimens do not hinder or block the propagation of shear bands during cyclic deformation. However, no shear band was observed in the UFG Ti either under tension or under cyclic deformation [17]. On the contrary, the surface was still smooth and there was no strain localization up to very late stage of cyclic deformation.

With further cyclic deformation, fatigue cracks always nucleated on the surface of the specimens, as shown in Fig. 9(c)–(f). Normally, the fatigue cracks often started at the corner of the specimen (Fig. 9(c)), then propagated along shear bands (see Fig. 9(d)), finally leading to a shear fracture through the whole specimen (see Fig. 9(e)). On the adjacent surface, the fatigue crack also occurred along the perpendicular shear bands (see Fig. 9(f)). This indicates that *the deformation* and damage of the ECAPed Al–0.7 wt.% Cu alloy mainly occur along the shear bands at the plastic strain amplitude below 10^{-3}, which is similar to PSB cracking in the fatigued copper single crystals [27]. The shear fatigue cracking is consistent with the observations in many other UFG metals [4,9–11] or alloys [2,15,16,20].

When the Al–0.7 wt.% Cu alloy was fatigued at the plastic strain amplitude over 10^{-3}, one group of coarse deformation

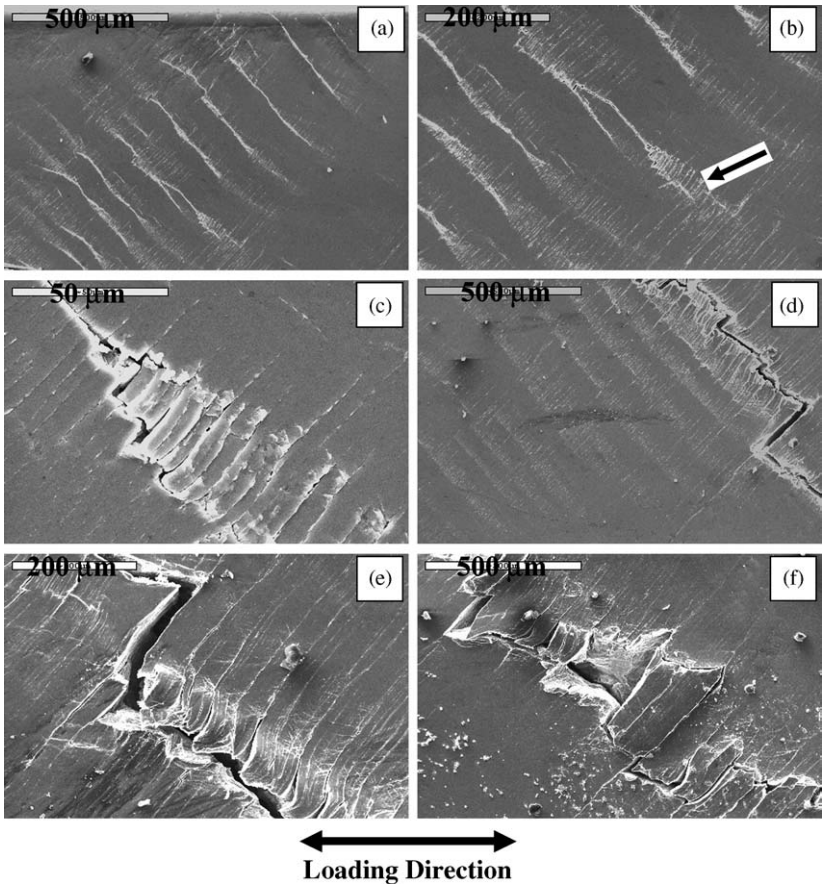

Fig. 10. Formation of coarse deformation bands and fatigue cracking along deformation bands at the plastic strain amplitude over 10^{-3}.

bands can be seen on the surface of the specimen, as shown in Fig. 10(a) and (b). The coarse deformation bands consist of regular shear bands with a width of tens to 200 μm, but it is different from the shear bands observed in Fig. 9 because of the following reasons: (1) the coarse deformation bands are wider than the shear bands; (2) the coarse deformation bands are not very straight and display a wavy feature; (3) the coarse deformation bands do not always transfer through the whole specimen, and often terminate at some sites of the surface. Besides, within the coarse deformation bands, there are many dense shear bands nearly approximately perpendicular to the deformation band direction. If the shear bands are compared to the persistent slip bands in the fatigued copper single crystals, the coarse deformation bands are quite similar to the deformation bands II [29]. The formation of deformation bands in fatigued copper single crystals is explained by locally irreversible rotation of crystal [30]. However, no crystallographic feature in the ECAPed Al–0.7 wt.% Cu alloy, the formation of the coarse deformation bands only depends on the applied strain amplitude rather than local crystallographic rotation. Therefore, the deformation mechanism of the UFG materials at high strain range must be different from that in single crystals and should be further revealed in the future.

Fatigue cracks can nucleate within the coarse deformation bands, as shown in Fig. 10(b) and (c). With further cyclic deformation, on a macro-scale, the fatigue crack often propagated along the coarse deformation bands, rather than the shear bands, as shown in Fig. 10(d) and (e). This result is well consistent with the fatigue cracking along the deformation bands II in copper single crystals fatigued at high strain ranges [29]. At local sites within the coarse deformation bands, the fatigue crack can propagate a small distance along the fine shear band, then switch its direction to the deformation band, showing a zigzag path on a macro-scale. Meanwhile, some small metal pieces scale off from the surface (see Fig. 10(f)) due to serious plastic strain incompatibility between shear bands and deformation band. From the observations above, the deformation and damage mechanisms of the ECAPed Al–0.7 wt.% Cu alloy in the applied plastic strain range can be illustrated in Fig. 11(a)–(d). Normally, fatigue cracking can either take place along the shear bands at low or medium strain range, or occur along the coarse deformation bands at high strain range, which has not been reported previously in UFG materials. It is suggested that fatigue cracking depends on the applied strain range or the degree of strain localization in the UFG materials. At high strain amplitude, the strain localization induced by pure shear deformation is insufficient to carry out the applied plastic strain. Consequently, a conjugated strain localization, approximately perpendicular to the shear bands, appeared in the form of the coarse deformation bands, which seemed to carry out more strain than the shear

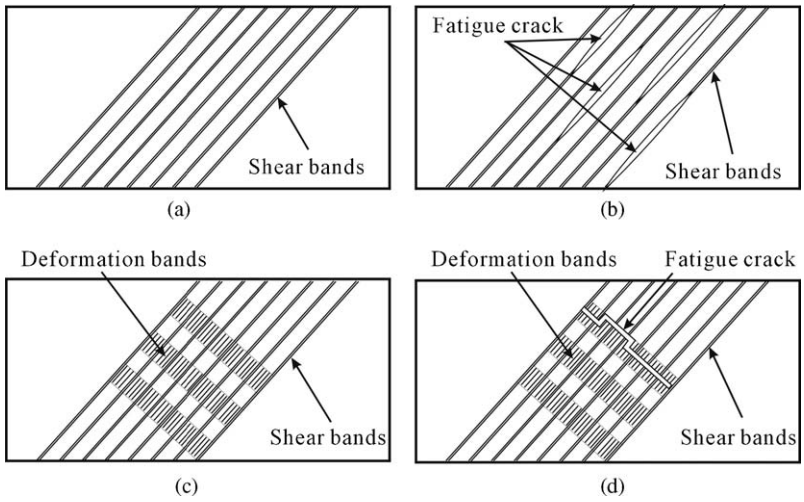

Fig. 11. Illustration of formation of (a, b) shear bands and fatigue cracking at low strain range; (c, d) the coarse deformation bands and fatigue cracking at high strain range.

bands, as shown in Figs. 9 and 10. Therefore, fatigue cracking is prone to nucleate along the coarse deformation bands rather than along the shear bands at high strain range. Meanwhile, the coarse deformation bands are basically parallel to the maximum shear stress plane of the specimen, which also fulfils the requirement in mechanics.

4. Conclusions

With increasing ECAP pass, the strength of the Al–0.7 wt.% Cu alloy increases. In comparison with pure Al, the addition of Cu element can also enhance the strength of the Al–0.7 wt.% Cu alloy after severe plastic deformation.

The Al–0.7 wt.% Cu alloy displays obvious cyclic softening behavior under constant plastic strain control. The fatigue life of the Al–0.7 wt.% Cu alloy is higher than the other Al alloys (Al–1.5Mg–Sc–Zr and Al–6Mg–0.5Sc–0.15Zr) subjected to severe plastic strain deformation.

The hysteresis energy density is high due to the obvious strengthening effect by ECAP treatment. The cyclic softening of the UFG materials can be attributed to the following reasons: (i) a relatively higher hysteresis energy density per cycle (due to high strength); (ii) a softening or stable deformation feature in the tensile stress–strain curves (no potential ability for strain strengthening); (iii) existence of mounts of dislocations and defects after ECAP treatment.

The plastic deformation of the ECAPed Al–0.7 wt.% Cu alloy was carried out either by shear bands only at low or medium strain range, or by shear bands and coarse deformation bands together at higher strain range. Consequently, fatigue cracks nucleated either along shear bands or along the coarse deformation bands, depending on the applied strain amplitude.

Acknowledgements

The authors would like to thank Yao G. and Wen J.L. for help during mechanical tests and Su H.H. and Gao W. for assistance with SEM observations. This work was supported by “Hundred of Talents Project” and the Special Funding for the National 100 Excellent Ph.D. Thesis by the Chinese Academy of Sciences, and National Natural Science Funding of China (NSFC) under grant No. 50371090.

References

[1] R.Z. Valiev, Mater. Sci. Eng. A234–A236 (1997) 59.
[2] C.S. Chung, J.K. Kim, H.K. Kim, W.J. Kim, Mater. Sci. Eng. A337 (2002) 39.
[3] H.W. Hoppel, R.Z. Valiev, Z. Metall. 93 (2002) 7.
[4] A. Vinogradov, S. Hashimoto, Adv. Eng. Mater. 5 (2003) 351.
[5] K. Neishi, Z. Horita, T.G. Langdon, Scripta Mater. 45 (2001) 965.
[6] R.Z. Valiev, R.K. Islamgaliev, I.V. Alexandrov, Prog. Mater. Sci. 45 (2000) 103.
[7] T.C. Lowe, Y.T. Zhu, Adv. Eng. Mater. 5 (2003) 373.
[8] S.R. Agnew, J.R. Weertman, Mater. Sci. Eng. A244 (1998) 145.
[9] H.W. Hoppel, Z.M. Zhou, H. Mughrabi, R.Z. Valiev, Philos. Mag. A82 (2002) 1781.
[10] S.D. Wu, Z.G. Wang, C.B. Jiang, G.Y. Li, R.Z. Valiev, Scripta Mater. 48 (2003) 1605.
[11] H. Mughrabi, H.W. Hoppel, M. Kautz, R.Z. Valiev, Z. Metall. 94 (2003) 1079.
[12] A. Vinogradov, S. Nagasaki, V. Patlan, K. Kitagawa, M. Kawazoe, Nanostruct. Mater. 11 (1999) 925.
[13] V. Patlan, A. Vinogradov, K. Higashi, K. Kitagawa, Mater. Sci. Eng. A300 (2001) 171.
[14] A. Vinogradov, A. Washikita, K. Kitagawa, V.I. Kopylov, Mater. Sci. Eng. A349 (2003) 318.
[15] S.M. Liu, Z.G. Wang, Scripta Mater. 48 (2003) 1421.
[16] A. Vinogradov, S. Hashimoto, V.I. Kopylov, Mater. Sci. Eng. A355 (2003) 277.
[17] A. Vinogradov, V.V. Stolyarov, S. Hshimoto, R.Z. Valiev, Mater. Sci. Eng. A318 (2001) 163.
[18] A. Vinogradov, V. Patlan, Y. Suzuki, K. Kitagawa, V.I. Kopylov, Acta Mater. 50 (2002) 1639.
[19] E. Thiele, C. Holste, H.K. Klemm, Z. Metall. 93 (2002) 730.
[20] H.K. Kim, M.I. Choi, C.S. Chung, D.H. Shin, Mater. Sci. Eng. A340 (2003) 243.
[21] Y. Iwahashi, Z. Horita, M. Nemoto, T.G. Longdon, Acta Mater. 45 (1997) 4733.

[22] L.J. Zheng, Ph.D. thesis, Northeastern University of China, 2002.
[23] D.R. Fang, Z.F. Zhang, S.D. Wu, C.X. Huang, H. Zhang, N.Q. Zhao, J.J. Li, submitted for publication.
[24] Z.F. Zhang, Z.G. Wang, Acta Mater. 46 (1998) 5063.
[25] H. Mughrabi, Mater. Sci. Eng. 33 (1978) 207.
[26] J. Polak, M. Klesnil, Mater. Sci. Eng. 63 (1984) 189.
[27] U. Essmann, U. Gosele, H. Mughrabi, Philos. Mag. 44 (1981) 405.
[28] B. Weiss, S. Kong, R. Stickler, L. Kunz, P. Lukas, Mater. Sci. Eng. A201 (1996) 65.
[29] Z.F. Zhang, Z.G. Wang, Z.M. Sun, Acta Mater. 49 (2001) 2875.
[30] X.W. Li, Z.G. Wang, S.X. Li, Philos. Mag. A80 (2000) 1901.